

## Article

# Thermal Migration Behavior of Na<sup>+</sup>, Cu<sup>2+</sup> and Li<sup>+</sup> in Montmorillonite

Zhenxiao Wu, Hao Zhao, Xuanping Zhou, Yang Wang, Kesheng Zuo \* and Hongfei Cheng \* 

School of Earth Science and Resources, Chang'an University, No. 126 Yanta Road, Xi'an 710054, China; 18331536081@163.com (Z.W.); haozhao1995@foxmail.com (H.Z.); zhouxuanping2021@163.com (X.Z.); yang.wang@chd.edu.cn (Y.W.)

\* Correspondence: keshengz@chd.edu.cn (K.Z.); h.cheng@chd.edu.cn (H.C.); Fax: +86-29-82339060 (K.Z. & H.C.)

**Abstract:** The main aim of this paper is to study the cation fixation sites in montmorillonite after heating at different temperatures. Montmorillonite was used to adsorb cations (Na<sup>+</sup>, Cu<sup>2+</sup> and Li<sup>+</sup>) in the solution, and the montmorillonite-adsorbed cations were heated at different temperatures (unheated, 100 °C, 200 °C and 300 °C) for 25 h. Subsequently, the basal spacing of montmorillonite treated at different temperatures was monitored by X-ray diffraction (XRD). The exchangeable cationic content (Na<sup>+</sup>, Cu<sup>2+</sup> and Li<sup>+</sup>) in montmorillonite was determined based on an inductively coupled plasma emission spectrometer (ICP-OES). In addition, the stretching and bending vibration changes in the OH group and the Si-O bond in montmorillonite were detected by Fourier transform infrared spectroscopy (FTIR). The vibration changes were related to the cation fixation sites. The XRD data showed that when the heating temperature reached 200 °C, the structure of montmorillonite adsorbing Li<sup>+</sup> and Cu<sup>2+</sup> ions completely collapsed, but the layer spacing of montmorillonite adsorbing Na<sup>+</sup> decreased slightly, which indicated that Li<sup>+</sup> and Cu<sup>2+</sup> were more easily able to enter the crystal structure. The ICP-OES results showed that the contents of exchangeable Na<sup>+</sup>, Cu<sup>2+</sup> and Li<sup>+</sup> in montmorillonite decreased with the increase in heating temperature, and Li<sup>+</sup> was more easily fixed by montmorillonite than Na<sup>+</sup> and Cu<sup>2+</sup>. The FTIR data showed that when montmorillonite adsorbed with Li<sup>+</sup> was heated at more than 200 °C, a new OH stretching vibration band appeared at 3971 cm<sup>-1</sup>, which may be caused by the migration of Li<sup>+</sup> into the octahedral vacancy to form a local trioctahedral structure. Na<sup>+</sup> has a large radius; it can only be fixed near the OH group and may not enter the tetrahedron/octahedron of montmorillonite. The number of charges carried by Cu<sup>2+</sup> is high and the dehydration enthalpy of hydrated Cu<sup>2+</sup> is high. When the heating temperature was greater than 200 °C, Cu<sup>2+</sup> mainly entered the hexagonal cavity of the tetrahedron and caused slight changes in the OH bending vibration. The vibration of the Si-O bond hardly changed after montmorillonite adsorbed Na<sup>+</sup>, but the stretching vibration peak of the Si-O bond moved to the high value region after adsorbing Cu<sup>2+</sup> and Li<sup>+</sup>, which was speculated to be related to the migration of Cu<sup>2+</sup> and Li<sup>+</sup> into the crystal structure.

**Keywords:** montmorillonite; cation; thermal migration; infrared



**Citation:** Wu, Z.; Zhao, H.; Zhou, X.; Wang, Y.; Zuo, K.; Cheng, H. Thermal Migration Behavior of Na<sup>+</sup>, Cu<sup>2+</sup> and Li<sup>+</sup> in Montmorillonite. *Minerals* **2022**, *12*, 477. <https://doi.org/10.3390/min12040477>

Academic Editor: Felix Brandt

Received: 22 March 2022

Accepted: 11 April 2022

Published: 13 April 2022

**Publisher's Note:** MDPI stays neutral with regard to jurisdictional claims in published maps and institutional affiliations.



**Copyright:** © 2022 by the authors. Licensee MDPI, Basel, Switzerland. This article is an open access article distributed under the terms and conditions of the Creative Commons Attribution (CC BY) license (<https://creativecommons.org/licenses/by/4.0/>).

## 1. Introduction

Montmorillonite is a typical layered silicate mineral, which is composed of two layers of silicon-oxygen tetrahedron and one layer of aluminium-oxygen octahedron. The octahedron of montmorillonite has the following two types: one is dioctahedral and only two-thirds of the cation coordination positions of the octahedron are filled with trivalent central atoms; the other is trioctahedral and the cation coordination positions of the octahedron are occupied by divalent cations [1–3]. The tetrahedral and octahedral layers of montmorillonite have a considerable degree of ion substitution. Si<sup>4+</sup> in the tetrahedral layer can be replaced by Al<sup>3+</sup> and Al<sup>3+</sup> in the octahedral layer can be replaced by Fe<sup>3+</sup>, Fe<sup>2+</sup>, Mg<sup>2+</sup>, etc., so that the structural unit layer has negative charges, which are balanced by exchangeable cations between structural unit layers and at the edge of unit layer [4–6]. Heating

montmorillonite at 200–300 °C would lead to the fixation of the exchangeable cations, the reduction in interlayer charge and the irreversible collapse of the mineral structure layer, behavior which is called the Hofmann-Klemen effect [7–9]. The final fixation sites of cations in minerals in the Hofmann-Klemen effect have been studied for more than 70 years, with no definitive answers [10,11]. There are three explanations for the Hofmann-Klemen effect, as follows: (i) cations migrate into the hexagonal cavity of the tetrahedral sheet [12,13]; (ii) the cation enters the vacancy in the octahedral sheet through the hexagonal channel of the tetrahedral sheet [14]; (iii) cation migration at both sites [15]. The exchangeable cations would remove the bound water on the surface during heating, and cations with small radii could be fixed in the mineral structure, resulting in the reduction in negative charge in the mineral layer [4].

Lithium ion ( $\text{Li}^+$ ) is one of the most common elements in the interlayer of montmorillonite and its ionic radius is small enough [4]. Relevant studies showed that the Hofmann-Klemen effect is likely caused by the interlayer  $\text{Li}^+$  migration into the lattice structure [4,9]. It is common to study the migration behavior of  $\text{Li}^+$  in heated montmorillonite. Luca et al. [13] used the  $^{57}\text{Fe}$  nucleus probe to detect the electronic disturbance of montmorillonite during heating. The results showed that  $\text{Li}^+$  would not enter the octahedral site. Gournis et al. [14] studied the lattice structure of lithium-saturated montmorillonite before and after heat treatment at 300 °C with neutron diffraction. The diffraction pattern showed that some Li were fixed in the octahedral sheet, and the rest remained in the interlayer space. Ebina et al. [15] calculated based on density functional theory (DFT) that  $\text{Li}^+$  in montmorillonite could migrate from the interlayer to the hexagonal cavity and the octahedral site when heated at 250–350 °C; the mobility is 60% and 40%, respectively. In addition, other scholars have studied the thermal migration behavior of other cations ( $\text{Ni}^{2+}$ ,  $\text{Zn}^{2+}$ ,  $\text{Mg}^{2+}$ ,  $\text{Cd}^{2+}$ ) [4,13,16–18], but there is still great controversy about whether the cations are fixed in the hexagonal cavity of the tetrahedral sheet or the previously vacant octahedral vacancy. Therefore, in this paper, three cations ( $\text{Li}^+$  with controversial fixed sites,  $\text{Cu}^{2+}$  with a similar radius to  $\text{Li}^+$  and  $\text{Na}^+$  with the same valence as  $\text{Li}^+$ ) are selected to explore the thermal migration behavior of interlayer cations in montmorillonite.

A large number of studies have used infrared spectroscopy to detect the fixed position of cations in clay [12,13,19]. When the molecule is irradiated with infrared light, the chemical bonds or functional groups in the molecule undergo vibration absorption. The absorption frequencies of different kinds of chemical bonds or functional groups are different; they would be in different positions in the infrared spectra, so as to obtain the information of internal chemical bonds or functional groups of clay minerals [20–22]. Fourier transform infrared spectroscopy (FTIR) has been widely used in the study of clay minerals.

Previous studies on the thermal migration behavior of single cations in clay have made some progress, but there are few studies on the fixed sites of different kinds of cations in montmorillonite [16,23,24]. Comparing the research results of different authors, it can be observed that the mineral structure, radius and charge of cations affect the cationic migration sites in clay minerals [7,23,25]. Therefore, based on infrared spectroscopy, the thermal migration behavior of different cations in montmorillonite was investigated in this study. The aim is to provide further reference information for the possible thermosetting sites of exchangeable cations in montmorillonite and to explore the influence of the types of cations on their thermosetting sites in clay minerals.

## 2. Experimental Section

### 2.1. Sample Preparation

The montmorillonite used in this study was purchased from Xianding Biotechnology Co., Ltd. (Shanghai, China). The  $\text{Li}^+$  solution,  $\text{Na}^+$  solution and  $\text{Cu}^{2+}$  solution used in the experiment were prepared from  $\text{Li}_2\text{SO}_4$  (AR),  $\text{Na}_2\text{SO}_4$  (AR) and  $\text{CuSO}_4$  (AR), respectively.

In order to remove the soluble impurities in montmorillonite, it was repeatedly washed with deionized water three times, then dried in an oven at 60 °C for 12 h and grinded into

powder in a mortar for standby. In order to prepare  $\text{Li}^+$ ,  $\text{Na}^+$  and  $\text{Cu}^{2+}$  montmorillonite (Li-MT, Na-MT and Cu-MT), 2.00 g of montmorillonite was immersed in 50 mL of  $\text{Li}^+$  (1 M),  $\text{Na}^+$  (1 M) and  $\text{Cu}^{2+}$  (1 M) solution, respectively, placed in an oscillator for about 2 h (50 r/min), and then the solid and liquid were separated by a filter. The separated solid was naturally dried at 20–25 °C. Through the above operations, a total of 4 groups of samples (Mt0, Mt100, Mt200 and Mt300) were prepared. Referring to the relevant literature, each group of samples was heated at a given temperature for 25 h (e.g., Mt0 for unheated samples and Mt100 for heating at 100 °C) [8,12,20].

## 2.2. Characterization

X-ray diffraction (XRD) was used to characterize the mineral composition in the sample, using an XRD-6100 (Shimadzu, Japan) with Cu-K $\alpha$  radiation ( $\lambda = 0.412$  nm) operating at 60 kV and 40 mA, with a  $2\theta$  scan range of 2° to 90° and scan rate of 4°/min.

The content of the exchangeable cations ( $\text{Cu}^{2+}$ ,  $\text{Na}^+$  and  $\text{Li}^+$ ) in the sample was determined by extraction with ammonium acetate solution (1 M) at pH 7. In step 1, 25 mg sample was dispersed in 5 mL of ethanol, then 5 mL of ammonium acetate solution was added, and the extract was collected after standing for 24 h. In step 2, 5 mL of deionized water was added to the remaining solid and the extract was collected after 24 h. In step 3, Step 1 and Step 2 were repeated three times. In step 4, the extracts of the same sample were mixed and the cation concentration in the solution was determined by the inductively coupled plasma emission spectrometer (ICP-OES, Agilent 5110, Santa Clara, CA, USA) [19].

The infrared spectra were obtained on a Fourier transform infrared spectra analyzer (PerkinElmer FTIR, Spectrum Two, Waltham, MA, USA) equipped with a DTGS detector. The samples to be tested (2 mg sample and 200 mg KBr) were prepared by KBr tablet pressing technology [8,19]. The samples were tested in the range of 4000–450  $\text{cm}^{-1}$ . The scanning times of each sample were 128  $\text{cm}^{-1}$  and the resolution was 4  $\text{cm}^{-1}$ .

The infrared spectra were usually divided into the following three regions: near infrared (NIR), medium infrared (MIR) and far infrared (FIR). The spectral vibrations of clay minerals in NIR (12,000–4000  $\text{cm}^{-1}$ ) include combination and overtone modes of the fundamental vibrations. The combined mode refers to the addition of two or more basic modes, and the overtone mode appears when a basic mode is excited by two or more quantum simultaneously [20]. The combination and overtone modes of water molecules appear at 5500–4500  $\text{cm}^{-1}$  and 7100–6000  $\text{cm}^{-1}$ , respectively. In clay minerals, the combination mode ( $\nu_{\text{OH}} + \sigma_{\text{OH}}$ ) and overtone mode ( $2\nu_{\text{OH}}$ ) of structural hydroxyl groups appear near 5000–4000  $\text{cm}^{-1}$  and 7000  $\text{cm}^{-1}$ , respectively [20]. There are few studies on montmorillonite FIR (400–10  $\text{cm}^{-1}$ ), mainly because it has no significant absorption bands in the region of 120–50  $\text{cm}^{-1}$  [20]. The thermal migration of cations in montmorillonite is mainly studied based on the vibration changes of OH groups, Si-O and Al-O in the mid-infrared region (4000–400  $\text{cm}^{-1}$ ) [20]. The vibration forms of OH groups include stretching vibration ( $\nu_{\text{OH}}$ ) and bending vibration ( $\sigma_{\text{OH}}$ ); the spectral regions are 3750–3000 and 950–600  $\text{cm}^{-1}$ , respectively. The stretching vibration of Si-O and Al-O is located at 1200–700  $\text{cm}^{-1}$ , and the bending vibration of Si-O and Al-O occurs in the spectral region of 600–400  $\text{cm}^{-1}$  [20].

Compared with NIR and FIR, MIR spectroscopy is more commonly used to study the mineral structure [26–28]. In addition, FTIR spectrometers collected in the MIR region are relatively cheap and available in most laboratories [20]. Therefore, in this experiment, the MIR spectroscopy was analyzed in detail to identify the fixed sites of exchangeable cations.

## 3. Results and Discussion

### 3.1. XRD Analysis

The montmorillonite used in this study has high purity and contains only a small amount of quartz and other impurities, and the XRD diffraction is shown in Figure 1. All the diffractions include both the basal reflections and the general  $hk$  diffractions of the montmorillonite. The characteristic of the basal reflection varies with the hydration

state of minerals. The general  $hk$  diffractions (marked with asterisks) are the structural characteristics of the montmorillonite layers themselves, which do not depend on interlayer hydration [11,25]. Moreover, the XRD patterns of montmorillonite after heating at different temperatures were studied. The  $hk$ -bank positions are the same in any sample and no new peaks that may be related to the new crystal structure were observed; whereas the basal reflection changes in the peak position.

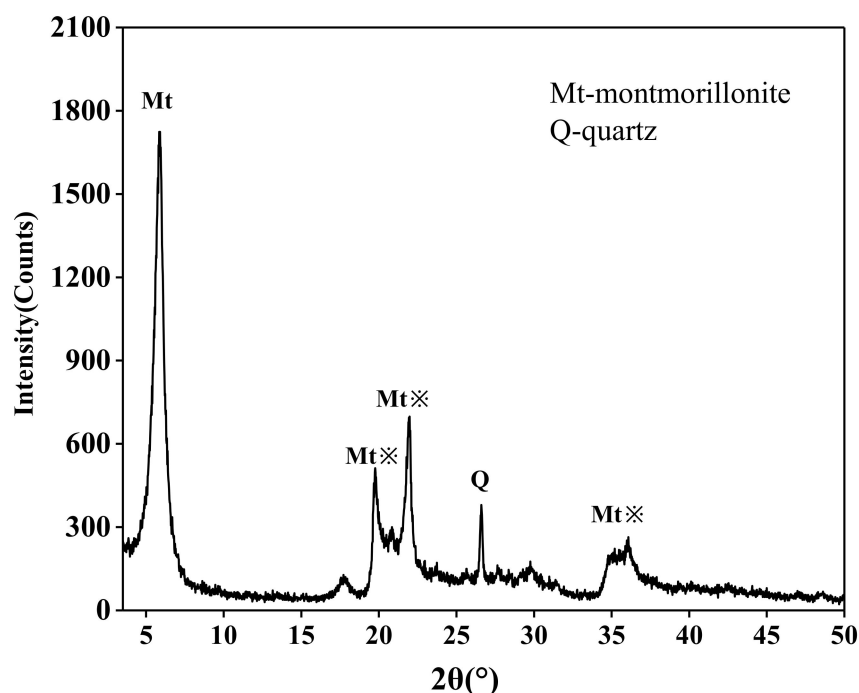


Figure 1. XRD patterns of montmorillonite.

The basal spacing of montmorillonite corresponds to its hydrated structure where hydrated cations are located in the interlayer space. Furthermore, the basal reflection peaks of montmorillonite are related to its chemical composition and the type of exchangeable cations [29]. The  $d_{001}$  spacing of unheated samples (Cu-Mt0, Na-Mt0 and Li-Mt0) were all in the range 13.1–14.4 Å (Table 1). The value of Li-Mt0 (13.1 Å) was slightly smaller than that of Na-Mt0 (14.4 Å) and Cu-Mt0 (14.1 Å), which was because the hydration degree of  $\text{Cu}^{2+}$  and  $\text{Na}^+$  was higher than that of  $\text{Li}^+$  [30]. Therefore, the interlayer spacing of  $\text{Cu}^{2+}$  and  $\text{Na}^+$  in the mineral interlayer was larger than that of  $\text{Na}^+$  in the interlayers.

Table 1. The  $d_{001}$  diffraction values of samples at different temperatures.

Heating Temperature (°C)	$d_{001}$ (Å)		
	Cu-Mt	Na-Mt	Li-Mt
unheated	14.1	14.4	13.1
100 °C	12.5	12.6	12.5
200 °C	9.7	12.6	9.9
300 °C	9.6	12.6	9.5

The  $d_{001}$  values of samples treated at 100 °C decreased slightly compared with unheated samples (Table 1). When the heating temperature was 200 °C, the layer spacings of Cu-Mt and Li-Mt were reduced to <10 Å, which was consistent with the thickness of the completely collapsed montmorillonite layer [11,25]. However, the layer spacing of Na-Mt was 12.6 Å, which indicated that the heat treatment would not lead to the complete collapse of the Na-Mt structure. There is an interaction between interlayer cations and the

aluminosilicate surface. The interlayer cation is positively charged and the aluminosilicate surface is negatively charged, which can produce electrostatic interactions [30,31]. When the cations were heated into the mineral crystal structure, it could reduce the negative charge carried by the aluminosilicate layers and reduce the spacing of mineral layers. It was inferred from the  $d_{001}$  values that  $\text{Li}^+$  and  $\text{Cu}^{2+}$  were more easily able to enter the mineral crystal structure than  $\text{Na}^+$ .

### 3.2. Exchangeable Cation Content

The contents of exchangeable  $\text{Cu}^{2+}$ ,  $\text{Na}^+$  and  $\text{Li}^+$  in the extract of montmorillonite heated at different temperatures were showed in Table 2. Compared with the exchangeable  $\text{Cu}^{2+}$  content in Cu-Mt0, Cu-Mt100, Cu-Mt200 and Cu-Mt300 decreased to 86.7%, 82.2% and 79.3%, respectively. The exchangeable  $\text{Na}^+$  in Na-Mt100, Na-Mt200 and Na-Mt300 decreased to 93.2%, 87.9% and 85.8% of Na-Mt0, respectively. The exchangeable  $\text{Li}^+$  in Li-Mt100, Li-Mt200 and Li-Mt300 decreased to 88.5%, 75.3% and 58.9% of Li-Mt0, respectively. The results showed that the content of exchangeable  $\text{Cu}^{2+}$ ,  $\text{Na}^+$  and  $\text{Li}^+$  in montmorillonite decreased with the increase in temperature. When heated to 100 °C, the content of exchangeable  $\text{Na}^+$  in montmorillonite changed little, while the content of exchangeable  $\text{Cu}^{2+}$  and  $\text{Li}^+$  decreased greatly. Further, when heated to 200 °C and 300 °C, the decrease rate of exchangeable  $\text{Li}^+$  in montmorillonite was significantly higher than that of  $\text{Na}^+$  and  $\text{Cu}^{2+}$ . In conclusion,  $\text{Li}^+$  was able to be fixed easier by montmorillonite than  $\text{Cu}^{2+}$  and  $\text{Na}^+$  during heating.

**Table 2.** Concentration of  $\text{Cu}^{2+}$ ,  $\text{Na}^+$  and  $\text{Li}^+$  in the extract.

Heating Temperature (°C)	Concentration (mg/L)		
	Cu-Mt	Na-Mt	Li-Mt
unheated	374.0	162.5	66.9
100 °C	324.5	151.4	59.2
200 °C	307.4	142.9	50.4
300 °C	296.4	139.5	39.4

### 3.3. FTIR Analysis

#### 3.3.1. OH Stretching Vibrations

The FTIR spectra of unheated samples (Na-Mt0, Cu-Mt0 and Li-Mt0) showed an obvious absorption band near  $3627\text{ cm}^{-1}$ , which was the OH group stretching vibration band coordinated with the central atom in the octahedron (Figure 2A–C). The stretching vibration of the OH group in montmorillonite is mainly affected by the following two factors: one is the nature of the central atom coordinated with hydroxyl in the octahedron; the other is isomorphism in the crystal. The top oxygen ( $\text{O}_{\text{ap}}$ ) of the tetrahedron can produce local negative charges. When the cations move into the crystal structure, which will neutralize the negative charges, it affects the stretching vibration of hydroxyl [19,32]. During the heating of Na-Mt, the stretching vibration band of OH remained near  $3627\text{ cm}^{-1}$  (Figure 2A). No displacement was detected in Cu-Mt100, and minimal displacement was observed in Cu-Mt200 and Cu-Mt300, ranging from  $3627$  to  $3631\text{ cm}^{-1}$ , respectively (Figure 2B). The stretching vibration change in OH in Li-Mt during heating was obviously different from that of Na-Mt and Cu-Mt. When heated to 100 °C, Li-Mt did not change; when the temperature continued to rise, the OH stretching vibration bands of Li-Mt200 and Li-Mt300 moved to  $3635\text{ cm}^{-1}$  and  $3640\text{ cm}^{-1}$ , respectively, and a new absorption band appeared at  $3671\text{ cm}^{-1}$  (Figure 2C). According to reports in the relevant literature, during the heating process of Li-Mt, hydrated  $\text{Li}^+$  can dehydrate into the empty octahedral site of montmorillonite to form a local trioctahedral structure ( $\text{AlMgLiOH}$ ), resulting in a new OH stretching vibration band at  $3671\text{ cm}^{-1}$  [19,20]. The experimental results showed that

$\text{Li}^+$  could enter the octahedral structure of montmorillonite, while  $\text{Cu}^{2+}$  and  $\text{Na}^+$  did not enter the octahedral structure of montmorillonite during heating.

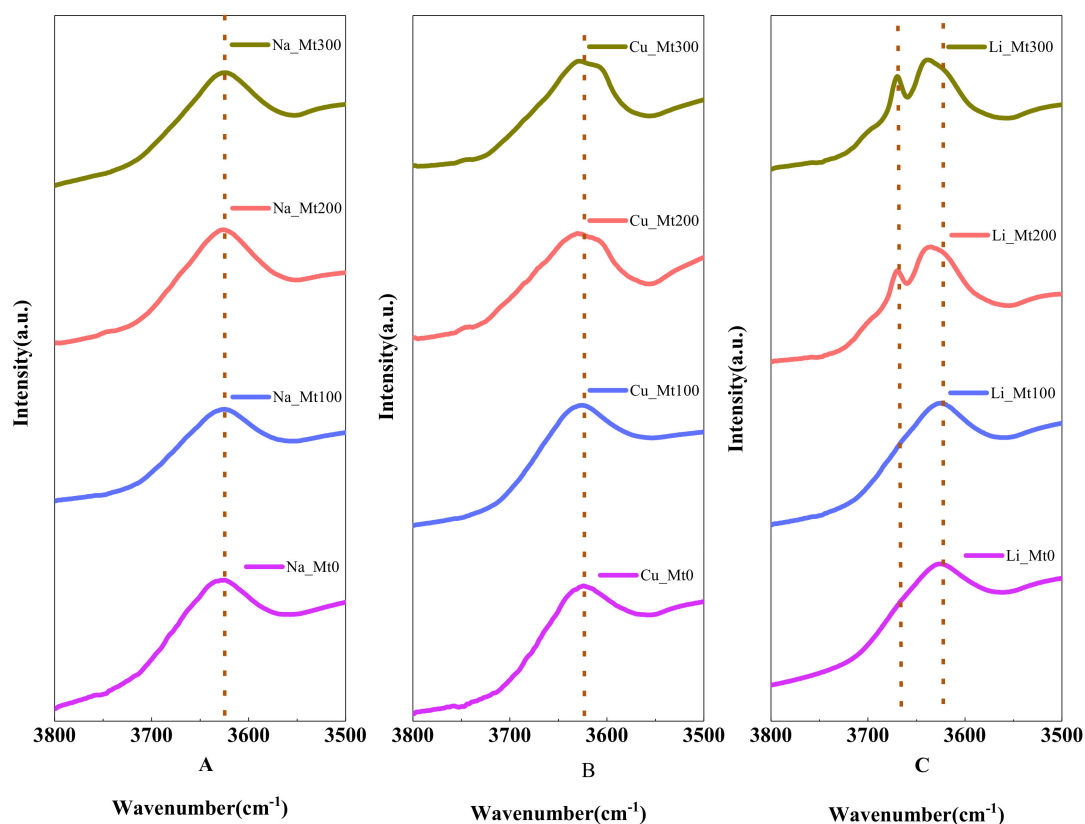


**Figure 2.** FTIR spectra of samples in OH stretching vibrations. (A) Na-Mt in different temperatures; (B) Cu-Mt in different temperatures; (C) Li-Mt in different temperatures.

It was shown that the cations entering the hexagonal cavity of clay minerals cause the OH stretching vibration band to move to a higher value [19,20]. For samples Li-Mt0, Na-Mt0 and Cu-Mt0, the charge imbalance in montmorillonite tetrahedral structure is caused by  $\text{O}_{\text{ap}}$ . When montmorillonite has a dioctahedral structure, OH and  $\text{O}_{\text{ap}}$  interact in the form of a hydrogen bond to form  $\text{OH}\cdots\text{O}_{\text{ap}}$ , and the interaction between O and H in OH is weakened [19]. When the cations migrate into the crystal structure, the negative charge of  $\text{O}_{\text{ap}}$  is balanced, the interaction between OH and  $\text{O}_{\text{ap}}$  is weakened, and the interaction between O and H in OH is enhanced, resulting in the movement of  $\nu_{\text{OH}}$  to a higher wavelength [19].

The movement of the OH stretching band is related to the properties (radius and charge) of interlayer cations. The radii of  $\text{Cu}^{2+}$ ,  $\text{Na}^+$  and  $\text{Li}^+$  are 0.72 Å, 0.95 Å and 0.68 Å, respectively [19,33]. Compared with  $\text{Li}^+$  and  $\text{Cu}^{2+}$ ,  $\text{Na}^+$  has a larger radius, which makes it unable to enter the hexagonal cavity/vacancy octahedron of montmorillonite. The radius difference between  $\text{Li}^+$  and  $\text{Cu}^{2+}$  is small, but the dehydration enthalpy of hydrated  $\text{Cu}^{2+}$  ( $-502 \text{ kcal mol}^{-1}$ ) is higher than that of hydrated  $\text{Li}^+$  ( $-124 \text{ kcal mol}^{-1}$ ); that is, hydrated  $\text{Cu}^{2+}$  ions are more difficult to dehydrate into the tetrahedral/octahedral structure of the crystal [20,23].

### 3.3.2. OH Bending Vibrations

The bending vibration of OH can further provide supplementary data for the migration behavior of cations during montmorillonite heating. The FTIR spectra of unheated samples (Li-Mt0, Na-Mt0 and Cu-Mt0) showed that there were obvious absorption bands near  $797 \text{ cm}^{-1}$ ,  $844 \text{ cm}^{-1}$  and  $912 \text{ cm}^{-1}$  (Figure 3A–C), which presumably correspond to the OH

group bending absorption bands of FeMgOH, AlMgOH and AlAlOH in minerals [34–36]. The absorption band at  $629\text{ cm}^{-1}$  may be caused by silicate impurities in the sample.

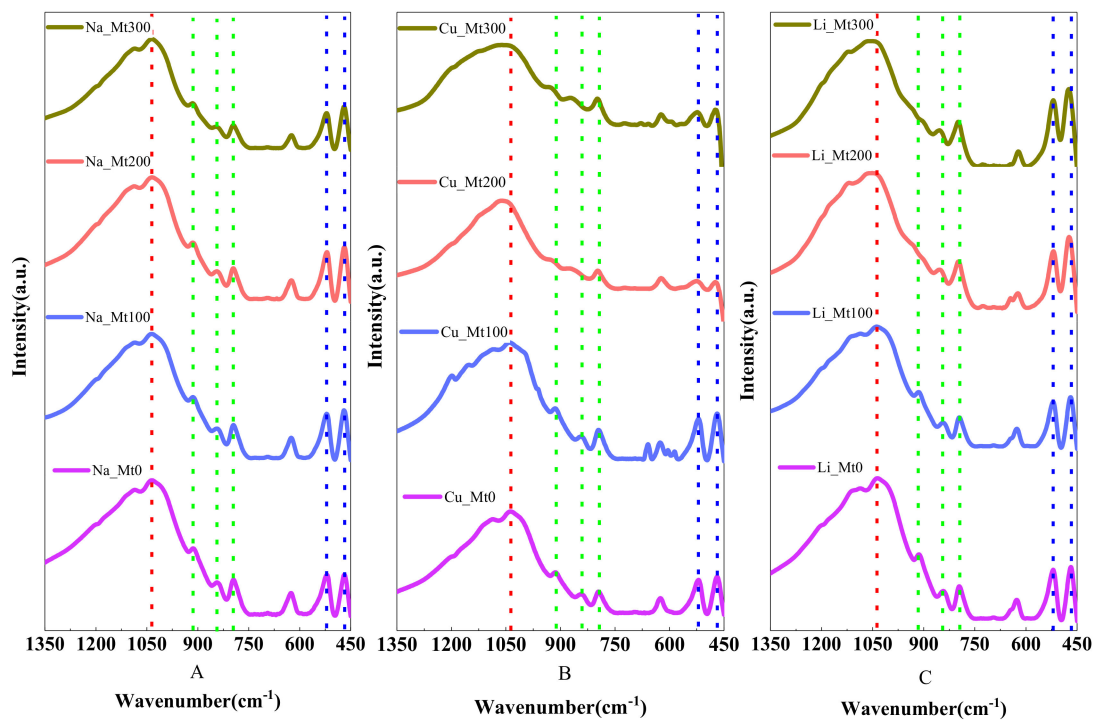


**Figure 3.** FTIR spectra of samples in OH bending vibrations (marked with green dotted line), Si-O stretching vibrations (marked with red dotted line) and Si-O bending vibrations (marked with blue dotted line). (A) Na-Mt in different temperatures; (B) Cu-Mt in different temperatures; (C) Li-Mt in different temperatures.

During the heating process of Na-Mt, the bending vibration of OH did not change significantly, and only the strength allocated to AlMgOH and AlAlOH in Na-Mt300 decreased slightly (Figure 3A). The radius of  $\text{Na}^+$  is larger and its hydrated ions cannot enter the hexagonal cavity of tetrahedron after dehydration, but the layer spacing of montmorillonite decreases when heated to  $300\text{ }^\circ\text{C}$ , making  $\text{Na}^+$  closer to the OH group, resulting in weak changes in the OH bending vibration band. Compared with Cu-Mt0, the OH bending vibration of Cu-Mt100 did not change (Figure 3B). When the heating temperature was further increased, the OH bending vibration band of Cu-Mt was weakened, the vibration peak of AlMgOH of Cu-Mt200 moved from  $844$  to  $868\text{ cm}^{-1}$  and the AlAlOH moved from  $912$  to  $925\text{ cm}^{-1}$ . The vibration peak of AlMgOH of Cu-Mt300 appeared at  $868\text{ cm}^{-1}$  and that of AlAlOH appeared at  $925\text{ cm}^{-1}$  (Figure 3B).  $\text{Cu}^{2+}$  can enter the hexagonal cavity of the tetrahedron during heating. The coulombic repulsion forces of  $\text{Cu}^{2+}$  may change the direction of the dipole moment of the OH group, thus interfering with the deformation vibration of the OH group. The infrared spectra of Li-Mt showed that when heated to  $200\text{ }^\circ\text{C}$  and  $300\text{ }^\circ\text{C}$ , the spectral peaks of AlMgOH appeared near  $850\text{ cm}^{-1}$  and the bending vibration of OH in AlAlOH was hardly observed (Figure 3C). The results showed that  $\text{Li}^+$  may migrate to the hexagonal cavity of the tetrahedron. According to the stretching vibration results of OH in Figure 2C, the migration site of  $\text{Li}^+$  is not singular and can exist in the tetrahedron and octahedron. Skoubris et al. [35] reported that during the heating process of montmorillonite, the hydrated  $\text{Li}^+$  between layers first migrated to the hexagonal cavity after dehydration, and then entered the vacancy octahedral site. In conclusion,  $\text{Na}^+$  cannot enter the hexagonal cavity during montmorillonite heating, but  $\text{Cu}^{2+}$  and  $\text{Li}^+$  can enter.

### 3.3.3. Si-O Vibrations

The interlayer cations in minerals migrate into the hexagonal cavities and/or the octahedral vacancies, which changes the stretching vibration and bending vibration of Si-O in the tetrahedral structure. The layer charge of minerals is balanced with the migration of cations, so that the mineral structure of montmorillonite is close to pyrophyllite (typical non-charged dioctahedral mineral) [33,37].

The Si-O stretching vibration peaks of Na-Mt0, Cu-Mt0 and Li-Mt0 were all located near  $1035\text{ cm}^{-1}$  (Figure 3). After heating, the Si-O stretching vibration of the Na-Mt series hardly changed (Figure 3A). Compared with Cu-Mt0, the Si-O band of Cu-Mt100 had no movement; when heated to  $200\text{ }^{\circ}\text{C}$ , the Si-O peak value moved from  $1035\text{ cm}^{-1}$  to  $1049\text{ cm}^{-1}$ ; when heated to  $200\text{ }^{\circ}\text{C}$ , the Si-O band widened and the peak moved to  $1050\text{ cm}^{-1}$  (Figure 3B). During the heating process of montmorillonite, the change trend of Li-Mt and Cu-Mt was similar. The Si-O stretching vibration band of Li-Mt100 was located near  $1037\text{ cm}^{-1}$  and its movement could be ignored (Figure 3C). The vibration peaks of Li-Mt200 and Li-Mt300 were  $1051\text{ cm}^{-1}$  and  $1053\text{ cm}^{-1}$ , respectively. During the heating process, the structure of montmorillonite became similar to pyrophyllite due to the migration of interlayer  $\text{Cu}^{2+}$  and  $\text{Li}^{+}$  (the Si-O stretching vibration peak of pyrophyllite was near  $1049\text{ cm}^{-1}$ ) [37].

The bending vibration bands of Si-O-Al and Si-O-Si of montmorillonite were located at  $520\text{ cm}^{-1}$  and  $467\text{ cm}^{-1}$ , respectively (Figure 3). During heating, the absorption bands of Na-Mt and Li-Mt did not change. Then, when heated to  $200\text{ }^{\circ}\text{C}$ , the Si-O bending vibration intensity of Cu-Mt decreased significantly. Compared with Cu-Mt, Li-Mt had no significant change, which may be due to its smaller valence state.

It was concluded that the cationic thermal migration in montmorillonite changes the bond length and Si-O<sub>basal</sub>-Si bond angle of the Si-O bond. Cu-Mt and Li-Mt change differently during heating, mainly due to the different fixation sites of  $\text{Cu}^{2+}$  and  $\text{Li}^{+}$  [38]. Even if  $\text{Cu}^{2+}$  and  $\text{Li}^{+}$  are located at the same site (for example, in a hexagonal cavity of a tetrahedron), their disturbance to Si-O is different. Compared with the divalent cations at the same site in the mineral structure, the electric field intensity of the monovalent cations is lower, so the disturbance to the Si-O bending vibration band is smaller [25,39].

## 4. Conclusions

In this paper, montmorillonite samples were characterized based on XRD, ICP-OES and FTIR in order to study the thermal migration of cations in the interlayer. The XRD data showed that  $\text{Li}^{+}$  and  $\text{Cu}^{2+}$  were more easily able to enter the crystal structure. This was because when the heating temperature reached  $200\text{ }^{\circ}\text{C}$ , the layer spacings of Cu-Mt and Li-Mt were  $<10\text{ \AA}$ , which was the layer spacing of completely collapsed montmorillonite, while the layer spacing of Na-Mt was only slightly reduced. Moreover, based on the study data of exchangeable cations in montmorillonite, the fixed content of cations increases as the temperature increases. In addition,  $\text{Li}^{+}$  was more easily fixed by montmorillonite than  $\text{Cu}^{2+}$  and  $\text{Na}^{+}$ .

It was found that the radius and charge of exchangeable cations affect their fixed sites in montmorillonite after heating. A new OH stretching vibration band at  $3971\text{ cm}^{-1}$  was observed in the heated Li-Mt200 and Li-Mt300, indicating that  $\text{Li}^{+}$  migrated to the octahedral vacancy and formed a local trioctahedral structure (AlMgLiOH). The radius of  $\text{Cu}^{2+}$  is similar to that of  $\text{Li}^{+}$ , but  $\text{Cu}^{2+}$  can only migrate into the hexagonal cavity of the tetrahedron because the charges carried by  $\text{Cu}^{2+}$  are higher and the dehydration enthalpy of hydrated  $\text{Cu}^{2+}$  is higher than that of hydrated  $\text{Li}^{+}$ .  $\text{Na}^{+}$  has a large radius and cannot penetrate the tetrahedron/octahedron. After heating and dehydration, interlayer hydrated  $\text{Na}^{+}$  could only be fixed near the OH group, causing slight changes in the bending vibration band of the OH group. The vibration results of the Si-O bond showed that Na-Mt hardly changes with the temperature increase. When Cu-Mt and Li-Mt were heated to  $200\text{ }^{\circ}\text{C}$ , the stretching vibration peak of the Si-O bond moved to the higher wavenumber region. In addition, the Si-O bond bending vibration bands of Na-Mt and Li-Mt did not change, but

the absorption band strength of Cu-Mt decreased, which may be due to the higher valence state of  $\text{Cu}^{2+}$  than that of  $\text{Li}^+$ .

**Author Contributions:** Writing—original draft preparation, Z.W.; writing—review and editing, H.C. and Y.W.; methodology, K.Z., H.Z. and X.Z. All authors have read and agreed to the published version of the manuscript.

**Funding:** This research was funded by the National Natural Science Foundation of China (Grant No. 42172043), Science and the Technology Major Projects of Shanxi Province of China (Grant No. 20181101003) and the Fundamental Research Funds for the Central Universities (Grant No. 300102299306, 300102271305).

**Institutional Review Board Statement:** Not applicable.

**Informed Consent Statement:** Not applicable.

**Data Availability Statement:** Data sharing is not applicable to this article.

**Acknowledgments:** The authors gratefully acknowledge the financial support provided by the National Natural Science Foundation of China (Grant No. 42172043), Science and the Technology Major Projects of Shanxi Province of China (Grant No. 20181101003) and the Fundamental Research Funds for the Central Universities (Grant No. 300102299306, 300102271305).

**Conflicts of Interest:** The authors declare no conflict of interest.

## References

1. Alshameri, A.; He, H.; Xin, C.; Zhu, J.; Xinghu, W.; Zhu, R.; Wang, H. Understanding the role of natural clay minerals as effective adsorbents and alternative source of rare earth elements: Adsorption operative parameters. *Hydrometallurgy* **2019**, *185*, 149–161. [[CrossRef](#)]
2. Alshameri, A.; He, H.; Zhu, J.; Xi, Y.; Zhu, R.; Ma, L.; Tao, Q. Adsorption of ammonium by different natural clay minerals: Characterization, kinetics and adsorption isotherms. *Appl. Clay Sci.* **2018**, *159*, 83–93. [[CrossRef](#)]
3. Bhattacharyya, K.G.; Gupta, S.S. Adsorption of a few heavy metals on natural and modified kaolinite and montmorillonite: A review. *Adv. Colloid Interface Sci.* **2007**, *140*, 114–131. [[CrossRef](#)]
4. Komadel, P.; Madejova, J.; Bujdak, J. Preparation and properties of reduced-charge smectites—A review. *Clays Clay Miner.* **2005**, *53*, 313–334. [[CrossRef](#)]
5. Pitteloud, C.; Powell, D.H.; Fischer, H.E. The hydration structure of the  $\text{Ni}^{2+}$  ion intercalated in montmorillonite clay: A neutron diffraction with isotopic substitution study. *Phys. Chem. Chem. Phys.* **2001**, *3*, 5567–5574. [[CrossRef](#)]
6. Adams, J.M. Synthetic organic chemistry using pillared, cation-exchanged and acid-treated montmorillonite catalysts—A review. *Appl. Clay Sci.* **1987**, *2*, 309–342. [[CrossRef](#)]
7. Haimovich, A.; Goldbourt, A. Characterization of lithium coordination sites with magic-angle spinning NMR. *J. Magn. Reson.* **2015**, *254*, 131–138. [[CrossRef](#)]
8. Seiffarth, T.; Kaps, C. Structural characterization of  $(\text{Cu}^{2+}, \text{Na}^+)$ - and  $(\text{Cu}^{2+}, \text{NH}_4^+)$ -exchanged bentonites upon thermal treatment. *Clays Clay Miner.* **2009**, *57*, 40–45. [[CrossRef](#)]
9. Hofmann, U.; Klemen, R. Verlust der austauschfähigkeit von lithiumionen an bentonit durch erhitzung. *Ztschrift Anorg. Und Allgemne Chem.* **1950**, *262*, 95–99. [[CrossRef](#)]
10. Emmerich, K.; Madsen, F.T.; Kahr, G. Dehydroxylation behavior of heat-treated and stream-treated homoionic Cis-vacant montmorillonites. *Clays Clay Miner.* **1999**, *47*, 591–604. [[CrossRef](#)]
11. Alba, M.D.; Alvero, R.; Becerro, A.I.; Castro, M.A.; Trillo, J.M. Chemical behavior of lithium ions in reexpanded Li-montmorillonites. *J. Phys. Chem. B* **1998**, *102*, 2207–2213. [[CrossRef](#)]
12. Bodart, P.R.; Delmotte, L.; Rigolet, S.; Brendlé, J.; Gougeon, R.D.  $^7\text{Li}\{^{19}\text{F}\}$  TEDOR NMR to observe the lithium migration in heated montmorillonite. *Appl. Clay Sci.* **2018**, *157*, 204–211. [[CrossRef](#)]
13. Luca, V.; Cardile, C.M. Thermally induced cation migration in Na and Li montmorillonite. *Phys. Chem. Miner.* **1988**, *16*, 98–103. [[CrossRef](#)]
14. Gournis, D.; Lappas, A.; Karakassides, M.A.; Többsen, D.; Moukarika, A. A neutron diffraction study of alkali cation migration in montmorillonites. *Phys. Chem. Miner.* **2008**, *35*, 49–58. [[CrossRef](#)]
15. Ebina, T.; Iwasaki, T.; Jee, A.C. XPS and DFT study on the migration of lithium in montmorillonite. *Clay Sci.* **2011**, *10*, 569–581.
16. Huve, L.; Delmotte, L.; Martin, P.; Dred, R.L.; Baron, J.; Saehr, D.  $^{19}\text{F}$  MAS-NMR study of structural fluorine in some natural and synthetic 2:1 layer silicates. *Clays Clay Miner.* **1992**, *40*, 186–191. [[CrossRef](#)]
17. Mosser, C.; Michot, L.J.; Villieras, E.; Romeo, M. Migration of cations in copper(II); exchanged montmorillonite and laponite upon heating. *Clays Clay Miner.* **1997**, *45*, 789–802. [[CrossRef](#)]
18. Sato, T. Effects of layer charge, charge location, and energy change on expansion properties of dioctahedral smectites. *Clays Clay Miner.* **1992**, *40*, 103–113. [[CrossRef](#)]

19. Madejová, J.; Arvaiová, B.; Komadel, P. FTIR spectroscopic characterization of thermally treated Cu<sup>2+</sup>, Cd<sup>2+</sup>, and Li<sup>+</sup> montmorillonites. *Spectrochim. Acta Part A Mol. Biomol. Spectrosc.* **1999**, *55*, 2467–2476. [[CrossRef](#)]
20. Madejová, J.; Pálková, H.; Komadel, P. Behaviour of Li<sup>+</sup> and Cu<sup>2+</sup> in heated montmorillonite: Evidence from far-, mid-, and near-IR regions. *Vib. Spectrosc.* **2006**, *40*, 80–88. [[CrossRef](#)]
21. Cao, Z.; Jia, Y.; Wang, Q.; Cheng, H. High-efficiency photo-Fenton Fe/g-C<sub>3</sub>N<sub>4</sub>/kaolinite catalyst for tetracycline hydrochloride degradation. *Appl. Clay Sci.* **2021**, *212*, 106213. [[CrossRef](#)]
22. Madejová, J. FTIR techniques in clay mineral studies. *Vib. Spectrosc.* **2003**, *31*, 1–10. [[CrossRef](#)]
23. Steudel, A.; Heinzmann, R.; Indris, S.; Emmerich, K. CEC and <sup>7</sup>Li MAS NMR study of interlayer Li<sup>+</sup> in the montmorillonite-beidellite series at room temperature and after heating. *Clays Clay Miner.* **2015**, *63*, 337–350. [[CrossRef](#)]
24. Wang, Y.; Cheng, H.; Hu, Q.; Liu, L.; Jia, L.; Gao, S.; Wang, Y. Pore structure heterogeneity of Wufeng-Longmaxi shale, Sichuan Basin, China: Evidence from gas physisorption and multifractal geometries. *J. Pet. Sci. Eng.* **2022**, *208*, 109313. [[CrossRef](#)]
25. Alvero, R.; Alba, M.D.; Castro, M.A.; Trillo, J.M. Reversible migration of lithium in montmorillonites. *Russ. J. Phys. Chem.* **1994**, *98*, 7848–7853. [[CrossRef](#)]
26. Cheng, J.; Zhang, J.; Xie, F.; Tuo, B.; Zhang, Y. Application and properties of organic emulsion coated phosphogypsum in aluminous rock based mineral polymer composite. *J. Wuhan Univ. Technol. Mater. Sci.* **2021**, *36*, 830–838. [[CrossRef](#)]
27. Wang, X.; Xu, X.; Ye, Y.; Wang, C.; Liu, D.; Shi, X.; Wang, S.; Zhu, X. In-situ high-temperature XRD and FTIR for calcite, dolomite and magnesite: Anharmonic contribution to the thermodynamic properties. *J. Earth Sci.* **2019**, *30*, 964–976. [[CrossRef](#)]
28. Hui, H.; Xu, Y.; Pan, M.E. On water in nominally anhydrous minerals from mantle peridotites and magmatic rocks. *Sci. China Earth Sci.* **2016**, *59*, 1157–1172. [[CrossRef](#)]
29. Ling, K.; Wen, H.; Zhang, Q.; Luo, C.; Gu, H.; Du, S.; Yu, W. Super-enrichment of lithium and niobium in the upper Permian Heshan Formation in Pingguo, Guangxi, China. *Sci. China Earth Sci.* **2021**, *64*, 753–772. [[CrossRef](#)]
30. Hrobáriková, J.; Madejová, J.; Komadel, P. Effect of heating temperature on Li-fixation, layer charge and properties of fine fractions of bentonites. *J. Mater. Chem.* **2001**, *11*, 1452–1457. [[CrossRef](#)]
31. Ma, L.; Zhu, J.; He, H.; Xi, Y.; Zhu, R.; Tao, Q.; Liu, D. Thermal analysis evidence for the location of zwitterionic surfactant on clay minerals. *Appl. Clay Sci.* **2015**, *112–113*, 62–67. [[CrossRef](#)]
32. Chouikhi, N.; Cecilia, J.A.; Vilarrasa-García, E.; Besghaier, S.; Chlendi, M.; Duro, F.I.F.; Castellon, E.R.; Bagane, M. CO<sub>2</sub> adsorption of materials synthesized from clay minerals: A review. *Minerals* **2019**, *9*, 514. [[CrossRef](#)]
33. Gao, X. *Clay Mineralogy*; Chemical Industry Press: Beijing, China, 2017.
34. Gates, W.P.; Komadel, P.; Madejová, J.; Bujdák, J.; Stucki, J.W.; Kirkpatrick, R.J. Electronic and structural properties of reduced-charge montmorillonites. *Appl. Clay Sci.* **2000**, *16*, 257–271. [[CrossRef](#)]
35. Skoubris, E.N.; Chryssikos, G.D.; Christidis, G.E.; Gionis, V. Structural characterization of reduced-charge montmorillonites. Evidence based on FTIR spectroscopy, thermal behavior, and layer-charge systematics. *Clay Clay Miner.* **2013**, *61*, 83–97.
36. Madejová, J.; Bujdák, J.; Petit, S.; Komadel, P. Effects of chemical composition and temperature of heating on the infrared spectra of Li-saturated dioctahedral smectites. (I) Mid-infrared region. *Clay Miner.* **2000**, *35*, 739–751.
37. Xia, L.; Zhong, H.; Liu, G.; Huang, Z.; Chang, Q.; Li, X. Comparative studies on flotation of illite, pyrophyllite and kaolinite with Gemini and conventional cationic surfactants. *Trans. Nonferrous Met. Soc. China* **2009**, *19*, 446–453. [[CrossRef](#)]
38. Karakassides, M.A.; Madejová, J.; Arvaiová, B.; Bourlinos, A.; Petridis, D.; Komadel, P. Location of Li(I), Cu(II) and Cd(II) in heated montmorillonite: Evidence from specular reflectance infrared and electron spin resonance spectroscopies. *J. Mater. Chem.* **1999**, *9*, 1553–1558. [[CrossRef](#)]
39. Clementz, D.M. Properties of reduced charge montmorillonite: Tetra-alkylammonium ion exchange forms. *Clays Clay Miner.* **1974**, *22*, 223–229. [[CrossRef](#)]